

NUMERICAL EVALUATION OF QUANTUM EFFECTS ON TRANSPORT CROSS SECTIONS*

by

S. Imam-Rahajoe, C. F. Curtiss, and R. B. Bernstein

University of Wisconsin, Theoretical Chemistry Institute
Madison, Wisconsin

29407

ABSTRACT

Quantum mechanical calculations of the transport cross sections $Q^{(1)*}$ and $Q^{(2)*}$ and the associated $\Omega^{(m,t)*}$ integrals are presented for a Lennard-Jones (12,6) potential. The computations are made for three values of the quantum parameter Λ^* ($=1, 2, 3$), and include the effects of statistics. The quantum effects become quite important at reduced temperatures T^* below about unity. The quantum corrections to the integrals are negative at moderate temperatures, but become positive at higher temperatures.

Author

* This research received financial support from Grant NsG-275-62 (4180) with the National Aeronautics and Space Administration and Contract AT(11-1)-1328 with the U.S. Atomic Energy Commission, Division of Research.

The theory of transport phenomena in a low density gas of structureless spherical molecules is well developed¹. The transport coefficients are given in terms of the temperature dependent reduced cross sections, $\Omega^{(m,t)*}$, which in turn are integrals of the energy dependent reduced cross sections, $\varphi^{(m)*}$. If quantum mechanics is used to describe the binary collisions between the molecules, these cross sections may be expressed in terms of the phase shifts, η_ℓ .

1. Cross Sections

In the present paper, we consider the quantum mechanical description of transport phenomena in a gas made up of molecules which interact according to a Lennard-Jones(12,6)potential

$$\psi(r) = \epsilon \varphi^*(r/\sigma) \quad 1-1$$

where

$$\varphi^*(r^*) = 4 \left[(r^*)^{-12} - (r^*)^{-6} \right] \quad 1-2$$

As usual, the constant ϵ is the depth of the potential minimum, the constant σ is the separation distance at which the potential is zero, and $r^* = r/\sigma$ is the reduced separation.

The phase shifts, η_ℓ , for collisions between molecules which interact according to the Lennard-Jones potential are obtained through the solution of the radial wave equation

$$\left\{ \frac{d^2}{dn^*{}^2} + \frac{4\pi^2}{\Lambda^*{}^2} [E^* - \varphi^*(n^*)] - \frac{\ell(\ell+1)}{n^*{}^2} \right\} n^* R_\ell(n^*) = 0 \quad 1-3$$

in which $R_\ell(n^*)$ is the radial wave function, $E^* = E/\epsilon$ is the reduced energy of the collision, and

$$\Lambda^* = h / (\sigma \sqrt{2\mu\epsilon}) \quad 1-4$$

is the "quantum parameter" which governs the magnitude of the quantum effects. The value of the phase shift is obtained from the asymptotic form of the solution of the wave equation which is finite at the origin and is a function of the angular momentum quantum number, ℓ , the reduced energy, E^* , and quantum parameter, Λ^* .

The two moments of the cross section which arise in the description of transport phenomena are $Q^{(1)}$ and $Q^{(2)}$. The corresponding reduced cross sections for collisions between unlike molecules (based on Boltzmann statistics) are

$$Q^{(1)*} = \frac{Q^{(1)}}{\pi \sigma^2} = \frac{\Lambda^*{}^2}{\pi^2 E^*} \sum_{\ell=0,1,2,\dots}^{\infty} (\ell+1) \sin^2(\eta_{\ell+1} - \eta_\ell) \quad 1-5$$

$$Q^{(2)*} = \frac{3 Q^{(2)}}{2\pi \sigma^2} = \frac{3 \Lambda^*{}^2}{2\pi^2 E^*} \sum_{\ell=0,1,2,\dots}^{\infty} \frac{(\ell+1)(\ell+2)}{(2\ell+3)} \sin^2(\eta_{\ell+2} - \eta_\ell) \quad 1-6$$

The expression for the cross section for collisions between like molecules depends on the statistics. The cross section $Q^{(1)}$ for collisions between like molecules does not appear in the

expressions for the transport coefficients. Neglecting spin effects, the reduced cross section $Q^{(2)*}$ for collisions between Bose-Einstein particles is

$$Q_{B.E.}^{(2)*} = \frac{3 \Lambda^*^2}{\pi^2 E^*} \sum_{l=0,2,4,\dots}^{\infty} \frac{(l+1)(l+2)}{(2l+3)} \sin^2(\eta_{l+2} - \eta_l) \quad 1-7$$

and for collisions between Fermi-Dirac particles is

$$Q_{F.D.}^{(2)*} = \frac{3 \Lambda^*^2}{\pi^2 E^*} \sum_{l=1,3,5,\dots}^{\infty} \frac{(l+1)(l+2)}{(2l+3)} \sin^2(\eta_{l+2} - \eta_l) \quad 1-8$$

For collisions between like atoms with nuclei of spin s the reduced cross sections are

$$[Q_{B.E.}^{(2)*}]^{(s)} = \left(\frac{s+1}{2s+1}\right) Q_{B.E.}^{(2)*} + \left(\frac{s}{2s+1}\right) Q_{F.D.}^{(2)*} \quad 1-9$$

$$[Q_{F.D.}^{(2)*}]^{(s)} = \left(\frac{s}{2s+1}\right) Q_{B.E.}^{(2)*} + \left(\frac{s+1}{2s+1}\right) Q_{F.D.}^{(2)*} \quad 1-10$$

The reduced cross sections, $Q^{(n)*}$, are functions of the reduced energy, E^* , the quantum parameter, Λ^* , and the statistics of the colliding pair.

The reduced temperature dependent cross sections, $\Omega^{(n,t)*}$, are simply integrals over the energy of the appropriate cross sections, $Q^{(n)*}$. Thus

$$\Omega^{(n,t)*} = [(t+1)! (\Lambda^*)^{t+2}]^{-1} \int_0^{\infty} Q^{(n)*} e^{-E^*/T^*} (E^*)^{t+1} dE^* \quad 1-11$$

where

$$T^* = k T / \epsilon \quad 1-12$$

is the reduced temperature. These cross sections are functions of the reduced temperature, T^* , the quantum parameter, Δ^* , and the statistics.

The expressions for the transport coefficients of single component systems and mixtures depend simply on the reduced cross sections, $\Omega^{(m,t)*}$. These expressions are given elsewhere¹ and are not repeated here.

2. Numerical Procedures

The phase shifts η_ℓ were computed by direct numerical integration (RKG method) of the radial wave equation using a program previously developed², but now improved by the introduction of a modification which continuously adjusted the integration interval depending upon the curvature of the wave function.

For convenience, the equivalences among the notation of references 1, 2, and the present discussion are summarized as follows:

$$x^* = n^* (\equiv n/\sigma) \quad 2-1$$

$$V(n) = \varphi(n) \quad 2-2$$

$$V^*(x) = \varphi^*(n^*) \quad (\equiv \varphi(n)/\epsilon) \quad 2-3$$

$$K = g^{*2} = E^* \quad (\equiv E/\epsilon) \quad 2-4$$

$$k = \hbar \quad (\equiv \mu g/\hbar = (2\mu E)^{1/2}/\hbar) \quad 2-5$$

$$A = k\sigma = \hbar\sigma \quad 2-6$$

$$B = (2\mu/\hbar^2)\epsilon\sigma^2 = A^2/K = 4\pi^2/\lambda^{*2} \quad 2-7$$

$$y = G_\ell(x)/\sigma = n^* R_\ell(n^*) \quad 2-8$$

The method of determination of the appropriate interval size is as follows. First, an initial interval size was chosen as the smaller of two quantities: $\Delta x_1 = \lambda/80\sigma$, where $\lambda = 2\pi/k$ is the de Broglie wavelength at $n = \infty$, and $\Delta x_2 = 1/40N$, where N is the number of nodes in the wave function due to the bound states³ ($N \approx \frac{\lambda}{2} + 0.27 B^{1/2}$). During the course of the integration, the interval size was varied so as to give approximately 40 integration intervals between two successive nodes.

The radial integration was stopped when the values of the "apparent phase shifts" calculated at four successive nodes differed from each other by less than 10^{-4} radian. The phases thus obtained were then used to calculate the transport cross sections, using eqs. 1-5, 1-7 and 1-8.

In the calculation of the transport cross sections, only $Q^{(1)*}$, $Q_{B.E.}^{(2)*}$, and $Q_{F.D.}^{(2)*}$ were calculated directly. The cross section $Q_{Boltz.}^{(2)*}$ was obtained from the simple relation

$$Q_{Boltz.}^{(2)*} = \frac{1}{2} (Q_{B.E.}^{(2)*} + Q_{F.D.}^{(2)*}) \quad 2-9$$

The calculations of the cross sections were carried out in the following way: For a given Λ^* and E^* , beginning with $\ell=0$, which subsequently was increased successively by unity, the program calculated the corresponding η_ℓ . After η_ℓ had been calculated, the program calculated the first term of the $Q^{(1)*}$ series; at $\ell=2$ the second term of $Q^{(1)*}$ and first term of $Q_{B.E.}^{(2)*}$; at $\ell=3$, the third term of $Q^{(1)*}$ and first term of $Q_{F.D.}^{(2)*}$; and so on. Hence, for each ℓ , except for $\ell=0$, the corresponding term was added to the $Q^{(1)*}$ series, and depending on whether ℓ was even or odd, terms of the $Q_{B.E.}^{(2)*}$ or $Q_{F.D.}^{(2)*}$ series, respectively, were added. The phases and corresponding partial sums of the $Q^{(n)*}$'s were printed out.

The calculation of the η_ℓ and $Q^{(n)*}$ was stopped when three consecutive partial sums of the $Q^{(n)*}$ series agreed to within .001, and the final ℓ was well beyond ℓ_n , the rainbow angular momentum⁴, i.e. $\eta < \eta_n$.

To calculate the reduced collision integrals $\Omega^{(m,t)*}$, the integral in eq. 1-11 was rewritten as

$$\Omega^{(m,t)*} = [(t+1)! (T^*)^{t+2}]^{-1} \int_0^\infty Q^{(n)*}(z) \exp[(t+2)z - \exp(z)/T^*] dz \quad 2-10$$

where $\mathbf{z} \equiv \ln E^*$. The integral was then evaluated by Weddle's rule⁵. In calculating the integrand, for $E^* \leq 1.0$ all $Q^{(n)*}$ values were computed directly, while for $E^* > 1$, some of the $Q^{(n)*}$ were interpolated in regions where the dependence of $Q^{(n)*}$ on \mathbf{z} was sufficiently smooth.

The range of values of E^* for which the $Q^{(n)*}$ were evaluated limited the range of values of T^* for which the $\Omega^{(n,t)*}$ could be evaluated. In order to estimate the maximum error due to the truncation of the range of numerical integration for the $\Omega^{(n,t)*}$ integrals, a simulated integration was carried out in which all of the $Q^{(n)*}$ within the range of integration were set equal to unity. Since the complete integral (with $Q^{(n)*} = 1$) is identically unity, the deviation of the above numerical result from unity served as an indication of the error due to the truncation. This procedure was carried out for various values of T^* so that limits could be established on the valid range of T^* .

The entire numerical procedure was carried out on the CDC 1604 computer at the University of Wisconsin Numerical Analysis Laboratory.

3. Results and Discussion

Figs. 1 and 2 show the dependence of $Q^{(1)*}$ (Boltzmann) and $Q^{(2)*}$ (Boltzmann) on E^* for $\Delta^* = 0, 1, 2$ and 3. The classical values ($\Delta^* = 0$) are those of Hirschfelder, Bird and Spotz⁶.

Fig. 3 shows the influence of the statistics upon $Q^{(2)*}$ for $\Delta^* = 1$. The $Q^{(n)*}$ have generally the expected negative energy dependence but superimposed on the smooth background is a pattern

of maxima which become more distinct under conditions such that a smaller number of terms contribute significantly to the sum. The origin of these resonances is the abrupt rise⁷ of the order of π in the phase shift for a particular value of ℓ which takes place over a more or less narrow range of energy. The sharpness of these peaks is related to $d\eta_\ell/dk$, or, more directly, to the collision lifetime⁸ $\tau_\ell = \hbar d\eta_\ell/dE$. The value of ℓ primarily responsible for each of the resonant peaks is indicated on the figures for the case of $\Delta^* = 1$. Similar maxima in the total cross section are expected⁹ and found experimentally from beam scattering studies¹⁰.

Figs. 4 and 5 show the dependence of $\Omega^{(1,1)}$ ^{*} (Boltzmann) and $\Omega^{(2,2)}$ ^{*} (Boltzmann) on T^* for $\Delta^* = 0, 1, 2$ and 3. The classical values ($\Delta^* = 0$) are those of Monchick and Mason¹¹. The $\Omega^{(m,t)}(T^*)$ curves are largely monotonic due to the averaging-out of the resonant peaks in $\Omega^{(n,t)}(T^*)$; however, some structure remains at sufficiently low temperatures for large Δ^* 's.

The high temperature behavior of $\Omega^{(1,1)}$ ^{*} and $\Omega^{(2,2)}$ ^{*} is illustrated in more detail in Figs. 6 and 7, where the percentage deviation from the classical values (the "quantum correction") is plotted vs. $T^{*-5/6}$ ¹². It has been shown by de Boer and Bird that in the almost classical limit ($\Delta^* \rightarrow 0$), this quantity, calculated for an inverse twelfth power repulsive potential, is positive and proportional to $\Delta^{*2} T^{*-5/6}$. It is to be expected that for the present case, i.e., the L.-J. (12,6) potential, the deviation function should approach this behavior in the limit of high temperature, but become negative at lower

temperature due to the influence of the attractive part of the potential.

In Figs. 6 and 7 the solid curves represent the results of the present calculation. The solid straight lines emanating from the origin show the expected limiting behavior for the Δ^* repulsive potential. The dashed lines indicate possible interpolations between the calculated and the limiting values. It is interesting to note from Fig. 7 that the crossing-over and changing of sign of the quantum correction is definitely established, at least for $\Delta^* = 3$.

the numerical values of the various $\Omega^{(n,t)*}$ integrals are presented in Tables 1 - 6. The classical values ($\Delta^* = 0$), of $\Omega^{(1,2)*}$, $\Omega^{(1,3)*}$, $\Omega^{(2,3)*}$ and $\Omega^{(2,4)*}$ are taken from Ref. 1, while those for $\Omega^{(1,1)*}$ and $\Omega^{(2,2)*}$ are the more recent values from Ref. 11. The present results (i.e., for $\Delta^* = 1, 2, 3$) are believed to be accurate to within ± 5 in the last digit.

It is of interest to note the rather sizeable magnitude of the quantum effects (see Figs. 4 and 5) even for T^* as high as unity. It thus appears that there are a number of physically interesting systems¹³ for which quantum effects on the transport properties cannot be considered merely "corrections" to the classical behavior.

Acknowledgment

One of us, S.I-R, would like to acknowledge the financial support of the Kentucky Research Foundation based on funds supplied by the U. S. Agency for International Development.

Figure Captions

Fig. 1. The influence of the quantum parameter, Λ^* , on the reduced cross section, $\Phi^{(1)}$.

Fig. 2. The influence of the quantum parameter, Λ^* , on the reduced cross section, $\Phi^{(2)}$.

Fig. 3. The effect of statistics on the reduced cross section, $\Omega^{(1)}$.

Fig. 4. The influence of the quantum parameter, Λ^* , on the integral $\Omega^{(1,1)}$.

Fig. 5. The influence of the quantum parameter, Λ^* , on the integral $\Omega^{(2,2)}$.

Fig. 6. The quantum correction to $\Omega^{(1,1)}$ in the high temperature region.

Fig. 7. The quantum correction to $\Omega^{(2,2)}$ in the high temperature region.

REFERENCES

1. J. O. Hirschfelder, C. F. Curtiss, and R. B. Bird, *Molecular Theory of Gases and Liquids* (John Wiley and Sons, Inc., New York, 1954; Second Printing, 1964).
2. R. B. Bernstein, *J. Chem. Phys.*, 33, 795 (1960).
3. H. Harrison and R. B. Bernstein, *J. Chem. Phys.*, 38, 2135 (1963).
4. K. W. Ford and J. A. Wheeler, *Ann. Phys.*, 7, 259 (1959).
5. R. A. Buckingham, *Numerical Methods*, (S.I. Pitman and Sons, Inc., London, 1957), p. 80.
6. J. O. Hirschfelder, R. B. Bird and E. L. Spotz, *J. Chem. Phys.*, 16, 968 (1948).
7. R. A. Buckingham and J. W. Fox, *Proc. Roy. Soc. (London)* A267, 102 (1962).
8. F. T. Smith, *Phys. Rev.*, 118, 349 (1960).
9. R. B. Bernstein, *J. Chem. Phys.*, 34, 361 (1961); 37, 1880 (1962).
10. See R. B. Bernstein, *Science*, 144, 141 (1964).
11. L. Monchick and E. A. Mason, *J. Chem. Phys.*, 35, 1676 (1961).
12. J. de Boer and R. B. Bird, *Physica* 20, 185 (1954); see also H. T. Wood and C. F. Curtiss, *J. Chem. Phys.*, 41, (1964).
13. Quantum calculations of $Q^{(1)*}$ and $Q^{(2)*}$ for CH_4 , Ne and T_2 have recently been reported by C. R. Mueller and J. W. Brackett, *J. Chem. Phys.*, 40, 654 (1964).

TABLE I
VALUES OF $\Omega^{(l,l)} *$

T^*	0	1	2	3
0.3	2.6494	2.8560	2.1970	1.1833
0.4	2.3144	2.4030	1.8158	1.1346
0.5	2.0661	2.0888	1.5954	1.0989
0.6	1.8767	1.8647	1.4529	1.0711
0.7	1.7293	1.6993	1.3534	1.0484
0.8	1.6122	1.5736	1.2800	1.0294
0.9	1.5175	1.4753	1.2235	1.0131
1.0	1.4398	1.3967	1.1786	0.9988
1.2	1.3204	1.2796	1.1115	0.9747
1.4	1.2336	1.1967	1.0632	0.9548
1.6	1.1679	1.1351	1.0265	0.9380
1.8	1.1166	1.0875	0.9974	0.9234
2.0	1.0753	1.0496	0.9735	0.9105
3.0	0.95003	0.9349	0.8962	0.8624
4.0	0.88453	0.8746	0.8511	0.8295
5.0	0.84277	0.8356	0.8198	0.8045
6.0	0.81287	0.8073	0.7960	0.7845
7.0	0.78976	0.7854	0.7768	0.7678
8.0	0.77111	0.7675	0.7608	0.7535

TABLE I (cont'd)

T*	0	1	2	3
9.0	0.75553	0.7525	0.7471	0.7411
10.0	0.74220	0.7396	0.7352	0.7301
11.0		0.7283	0.7246	0.7202
12.0	0.72022	0.7182	0.7150	0.7112
13.0		0.7091	0.7064	0.7031
14.0	0.70254	0.7009	0.6985	0.6956
15.0		0.6933	0.6913	0.6886
16.0	0.68776	0.6864	0.6846	0.6822
17.0		0.6799	0.6783	0.6762
18.0	0.67510	0.6739	0.6725	0.6705
19.0			0.6670	0.6652
20.0	0.66405		0.6618	0.6602
21.0			0.6570	0.6555
22.0			0.6524	0.6510
23.0			0.6480	0.6467
24.0			0.6438	0.6426
25.0	0.64136		0.6398	0.6387
26.0			0.6360	0.6350
27.0			0.6324	0.6314
28.0			0.6289	0.6280

TABLE II
VALUES OF $\Omega^{(1,2)} *$

T^*	0	1	2	3
0.3	2.256	2.3136	1.6792	1.1254
0.4	1.931	1.9045	1.4425	1.0799
0.5	1.705	1.6511	1.3067	1.0470
0.6	1.543	1.4832	1.2185	1.0213
0.7	1.423	1.3655	1.1563	1.0003
0.8	1.332	1.2791	1.1099	0.9826
0.9	1.261	1.2132	1.0736	0.9674
1.0	1.204	1.1614	1.0443	0.9540
1.2	1.119	1.0853	0.9994	0.9312
1.4	1.059	1.0318	0.9661	0.9124
1.6	1.013	0.9920	0.9400	0.8964
1.8	0.9780	0.9609	0.9187	0.8824
2.0	0.9500	0.9358	0.9009	0.8701
3.0	0.8640	0.8567	0.8401	0.8237
4.0	0.8167	0.8119	0.8023	0.7918
5.0	0.7847	0.7813	0.7749	0.7676
6.0	0.7607	0.7581	0.7537	0.7481
7.0	0.7420	0.7396	0.7362	0.7320
8.0	0.7260	0.7241	0.7216	0.7181

TABLE II (cont'd)

T*	0	1	2	3
9.0	0.7127	0.7109	0.7089	0.7061
10.0	0.7013	0.6994	0.6977	0.6954
11.0		0.6892	0.6878	0.6858
12.0		0.6800	0.6789	0.6771
13.0		0.6717	0.6707	0.6692
14.0		0.6641	0.6633	0.6620
15.0		0.6572	0.6564	0.6552
16.0			0.6501	0.6490
17.0			0.6441	0.6432
18.0			0.6386	0.6377
19.0			0.6334	0.6326
20.0	0.6293		0.6285	0.6277
21.0			0.6238	0.6231
22.0			0.6194	0.6188
23.0			0.6152	0.6147
24.0			0.6113	0.6107

TABLE III
VALUES OF $\Omega^{(1,3)}$

T^*	0	1	2	3
0.3	1.962	1.9194	1.4363	1.0843
0.4	1.663	1.5893	1.2699	1.0419
0.5	1.468	1.3977	1.1731	1.0110
0.6	1.336	1.2752	1.1092	0.9868
0.7	1.242	1.1909	1.0634	0.9668
0.8	1.172	1.1295	1.0285	0.9499
0.9	1.119	1.0828	1.0007	0.9353
1.0	1.076	1.0459	0.9779	0.9224
1.2	1.013	0.9912	0.9422	0.9004
1.4	0.9680	0.9520	0.9150	0.8822
1.6	0.9345	0.9222	0.8933	0.8666
1.8	0.9082	0.8985	0.8752	0.8530
2.0	0.8867	0.8790	0.8598	0.8410
3.0	0.8187	0.8145	0.8056	0.7956
4.0	0.7790	0.7759	0.7708	0.7644
5.0	0.7510	0.7485	0.7452	0.7407
6.0	0.7295	0.7273	0.7250	0.7217
7.0	0.7120	0.7101	0.7084	0.7059
8.0	0.6973	0.6957	0.6944	0.6924

TABLE III (cont'd)

T^*	0	1	2	3
9.0	0.6847	0.6833	0.6822	0.6806
10.0	0.6735	0.6724	0.6715	0.6702
11.0		0.6627	0.6619	0.6608
12.0		0.6539	0.6533	0.6523
13.0			0.6455	0.6446
14.0			0.6383	0.6375
15.0			0.6317	0.6310
16.0			0.6255	0.6249
17.0			0.6198	0.6192
18.0			0.6144	0.6139
19.0			0.6094	0.6089
20.0	0.6048		0.6046	0.6042

TABLE IV
 ∇ VALUES OF $\Omega^{(2,2)}$

T^*	0 Boltz.	1 B.E.	2 Boltz.	3 Boltz.
0.3	2.8399	3.1262	3.1294	3.1326
0.4	2.5310	2.6400	2.6400	2.6400
0.5	2.2837	2.2935	2.2930	2.2924
0.6	2.0838	2.0434	2.0430	2.0424
0.7	1.9220	1.8582	1.8578	1.8574
0.8	1.7902	1.7172	1.7169	1.7166
0.9	1.6823	1.6074	1.6071	1.6069
1.0	1.5929	1.5199	1.5196	1.5194
1.2	1.4551	1.3902	1.3900	1.3898
1.4	1.3551	1.2994	1.2992	1.2990
1.6	1.2800	1.2325	1.2324	1.2322
1.8	1.2219	1.1814	1.8122	1.1811
2.0	1.1757	1.1409	1.1408	1.1407
3.0	1.0388	1.0209	1.0208	1.0207
4.0	0.96988	0.9593	0.9592	0.9591
5.0	0.92676	0.9197	0.9196	0.9195
6.0	0.89616	0.8911	0.8910	0.8910

TABLE IV (cont'd)

T^*	0 Boltz.	0 B.E.	1 Boltz.	1 F.D.	B.E.	2 Boltz.	2 F.D.	B.E.	3 Boltz.	F.D.
7.0	0.87272	0.8688	0.8688	0.8687	0.8642	0.8641	0.8640	0.8626	0.8625	0.8625
8.0	0.85379	0.8507	0.8506	0.8506	0.8475	0.8475	0.8474	0.8469	0.8469	0.8468
9.0	0.83795	0.8354	0.8354	0.8353	0.8332	0.8332	0.8331	0.8332	0.8332	0.8332
10.0	0.82435	0.8221	0.8221	0.8222	0.8207	0.8206	0.8205	0.8212	0.8211	0.8211
11.0	0.8105	0.8105	0.8106	0.8096	0.8095	0.8094	0.8103	0.8103	0.8103	0.8103
12.0	0.80184	0.8001	0.8002	0.8002	0.7996	0.7995	0.7994	0.8005	0.8005	0.8005
13.0	0.7908	0.7908	0.7908	0.7908	0.7905	0.7904	0.7903	0.7916	0.7916	0.7916
14.0	0.78363	0.7823	0.7823	0.7823	0.7822	0.7821	0.7820	0.7834	0.7833	0.7833
15.0	0.76834				0.7746	0.7745	0.7744	0.7758	0.7757	0.7757
16.0	0.75518				0.7675	0.7674	0.7673	0.7687	0.7687	0.7687
17.0					0.7608	0.7607	0.7607	0.7621	0.7621	0.7621
18.0					0.7546	0.7545	0.7545	0.7559	0.7559	0.7559
19.0					0.7488	0.7487	0.7487	0.7501	0.7501	0.7501
20.0	0.74364				0.7433	0.7433	0.7432	0.7446	0.7446	0.7446
21.0					0.7381	0.7381	0.7380	0.7394	0.7394	0.7394
22.0					0.7332	0.7331	0.7331	0.7345	0.7345	0.7344
23.0					0.7285	0.7285	0.7284	0.7298	0.7298	0.7297
24.0					0.7241	0.7240	0.7240	0.7253	0.7253	0.7253

TABLE V
VALUES OF $\Omega^{(2,3)}$

T^*	0	1	2	3
	Boltz.	B.E.	Boltz.	B.E.
0.3	2.535	2.6987	2.6971	2.6955
0.4	2.232	2.2315	2.2303	2.2290
0.5	1.992	1.9286	1.9280	1.9273
0.6	1.806	1.7232	1.7229	1.7225
0.7	1.661	1.5775	1.5773	1.5770
0.8	1.549	1.4700	1.4698	1.4696
0.9	1.460	1.3880	1.3878	1.3877
1.0	1.388	1.3237	1.3235	1.3234
1.2	1.280	1.2297	1.2296	1.2294
1.4	1.205	1.1645	1.1644	1.1643
1.6	1.149	1.1166	1.1165	1.1163
1.8	1.106	1.0798	1.0796	1.0795
2.0	1.073	1.0504	1.0503	1.0501
3.0	0.9708	0.9606	0.9605	0.9604
4.0	0.9175	0.9115	0.9114	0.9113
5.0	0.8823	0.8784	0.8784	0.8783

TABLE V (cont'd)

T	0			1			2			3		
	A* Boltz.	B.E.	Boltz.	F.D.	B.E.	Boltz.	F.D.	B.E.	Boltz.	F.D.	Boltz.	F.D.
6.0	0.8565	0.8537	0.8536	0.8536	0.8512	0.8511	0.8510	0.8509	0.8509	0.8508		
7.0	0.8360	0.8339	0.8339	0.8339	0.8325	0.8325	0.8324	0.8330	0.8330	0.8330		
8.0	0.8193	0.8175	0.8175	0.8175	0.8168	0.8167	0.8166	0.8177	0.8177	0.8177		
9.0	0.8048	0.8035	0.8035	0.8035	0.8032	0.8032	0.8031	0.8044	0.8044	0.8044		
10.0	0.7923	0.7913	0.7913	0.7913	0.7913	0.7912	0.7911	0.7926	0.7926	0.7926		
11.0	0.7804	0.7804	0.7804	0.7804	0.7807	0.7806	0.7805	0.7821	0.7821	0.7820		
12.0	0.7707	0.7707	0.7707	0.7707	0.7711	0.7710	0.7709	0.7725	0.7725	0.7725		
13.0					0.7623	0.7622	0.7622	0.7638	0.7637	0.7637		
14.0					0.7543	0.7542	0.7542	0.7557	0.7557	0.7557		
15.0					0.7469	0.7468	0.7468	0.7483	0.7483	0.7483		
16.0					0.7401	0.7400	0.7399	0.7414	0.7414	0.7414		
17.0					0.7336	0.7336	0.7335	0.7350	0.7350	0.7350		
18.0					0.7276	0.7276	0.7275	0.7289	0.7289	0.7289		
19.0					0.7220	0.7219	0.7219	0.7232	0.7232	0.7232		
20.0					0.7166	0.7166	0.7165	0.7179	0.7179	0.7179		
					0.7160							

TABLE VI
VALUES OF $\Omega^{(2,4)}$

τ^*	0	1	2	3						
T^*	Boltz.	B.E.	Boltz.	F.D.	B.E.	Boltz.	F.D.	B.E.	Boltz.	F.D.
0.3	2.333	2.3499	2.3477	2.3456	1.6731	1.6805	1.6880	1.3880	1.2522	1.1164
0.4	2.016	1.9349	1.9343	1.9336	1.4752	1.4743	1.4734	1.2109	1.2006	1.1904
0.5	1.781	1.6827	1.6825	1.6823	1.3544	1.3536	1.3528	1.1490	1.1625	1.1760
0.6	1.610	1.5181	1.5179	1.5178	1.2746	1.2742	1.2738	1.1210	1.1326	1.1443
0.7	1.484	1.4040	1.4038	1.4037	1.2177	1.2175	1.2173	1.1016	1.1083	1.1150
0.8	1.389	1.3210	1.3208	1.3207	1.1748	1.1746	1.1745	1.0846	1.0879	1.0911
0.9	1.316	1.2582	1.2580	1.2579	1.1409	1.1407	1.1406	1.0689	1.0703	1.0717
1.0	1.258	1.2091	1.2089	1.2088	1.1133	1.1131	1.1129	1.0544	1.0549	1.0554
1.2	1.174	1.1374	1.1372	1.1371	1.0705	1.0702	1.0699	1.0291	1.0291	1.0290
1.4	1.115	1.0873	1.0871	1.0870	1.0384	1.0380	1.0377	1.0079	1.0078	1.0077
1.6	1.072	1.0500	1.0499	1.0497	1.0130	1.0127	1.0124	0.9899	0.9899	0.9898
1.8	1.038	1.0210	1.0209	1.0207	0.9922	0.9919	0.9916	0.9744	0.9743	0.9743
2.0	1.012	0.9975	0.9974	0.9973	0.9747	0.9744	0.9742	0.9607	0.9607	0.9606
3.0	0.9295	0.9231	0.9230	0.9230	0.9143	0.9142	0.9141	0.9098	0.9097	0.9096
4.0	0.8840	0.8802	0.8802	0.8801	0.8762	0.8762	0.8761	0.8749	0.8749	0.8748
5.0	0.8530	0.8503	0.8503	0.8502	0.8484	0.8484	0.8483	0.8486	0.8486	0.8486

TABLE VI (cont'd)

$\frac{\lambda^*}{T}$	0	1	2	3
	Boltz.	B.E.	Boltz.	B.E.
6.0	0.8295	0.8274	0.8274	0.8266
7.0	0.8105	0.8089	0.8089	0.8087
8.0	0.7945	0.7934	0.7935	0.7934
9.0	0.7810	0.7800	0.7801	0.7803
10.0	0.7690	0.7683	0.7684	0.7688
11.0	0.7578	0.7579	0.7579	0.7584
12.0			0.7491	0.7490
13.0			0.7406	0.7405
14.0			0.7328	0.7327
15.0			0.7256	0.7255
16.0			0.7188	0.7188
17.0			0.7126	0.7125

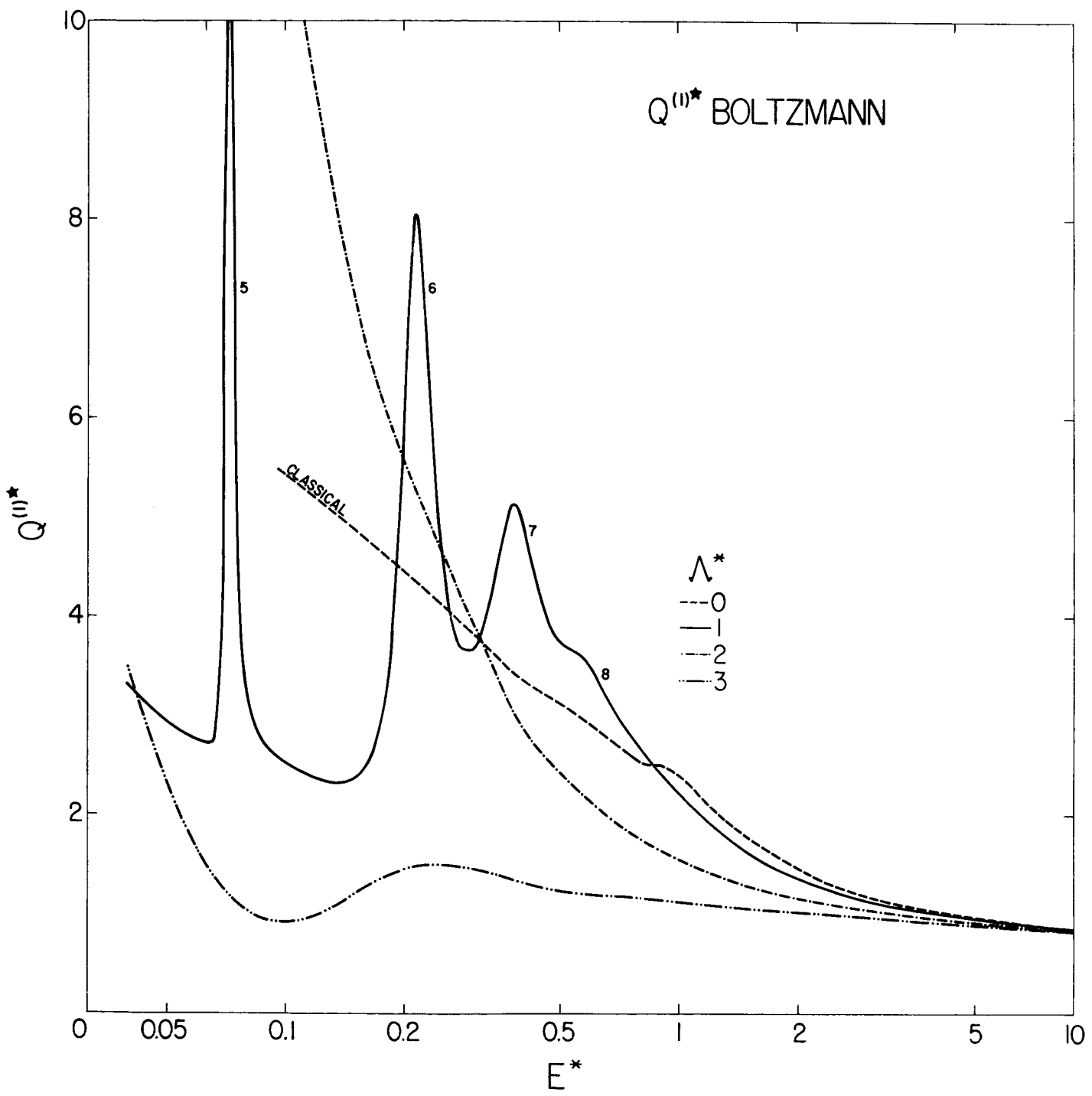


FIG. I

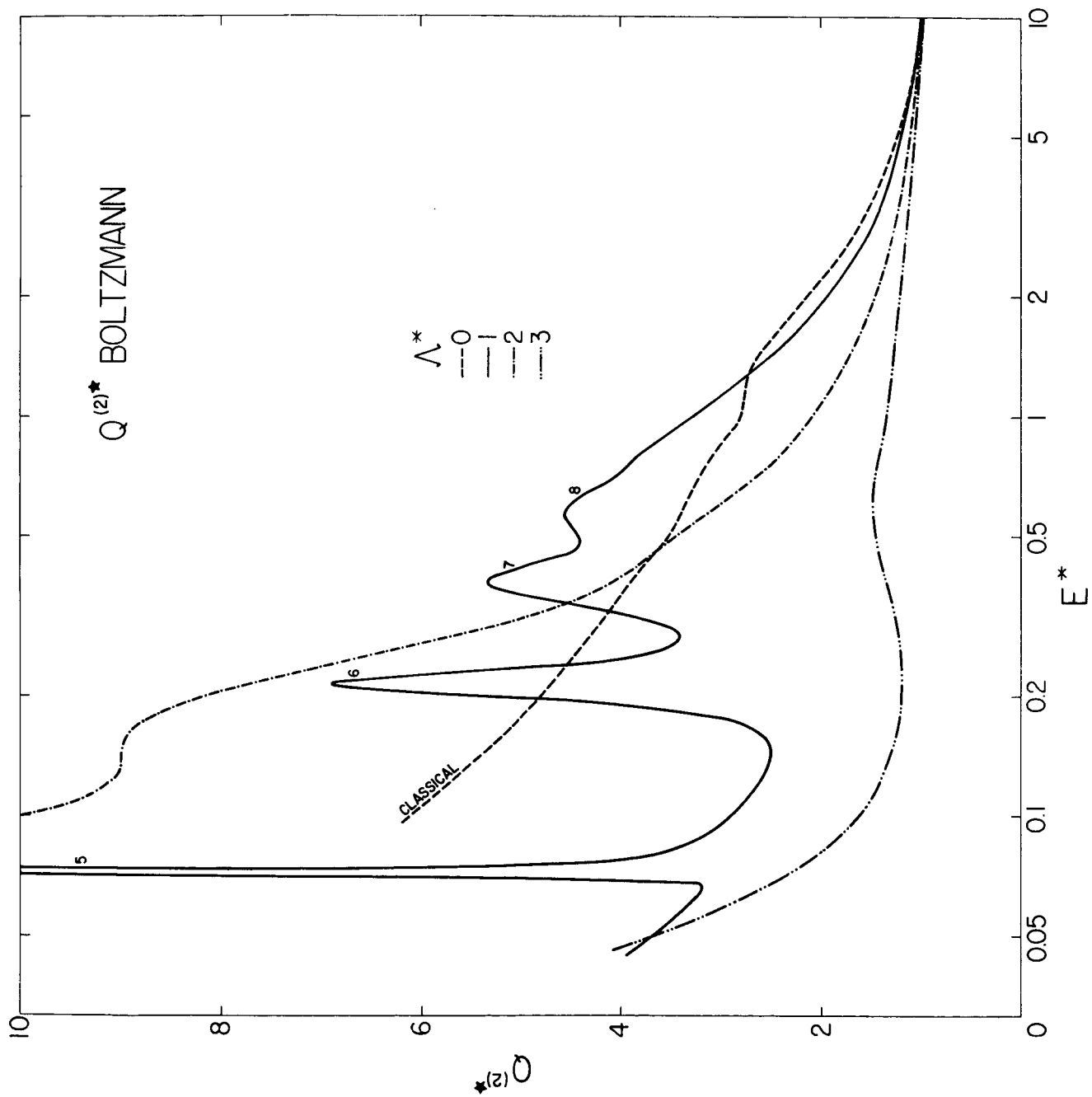


FIG. 2

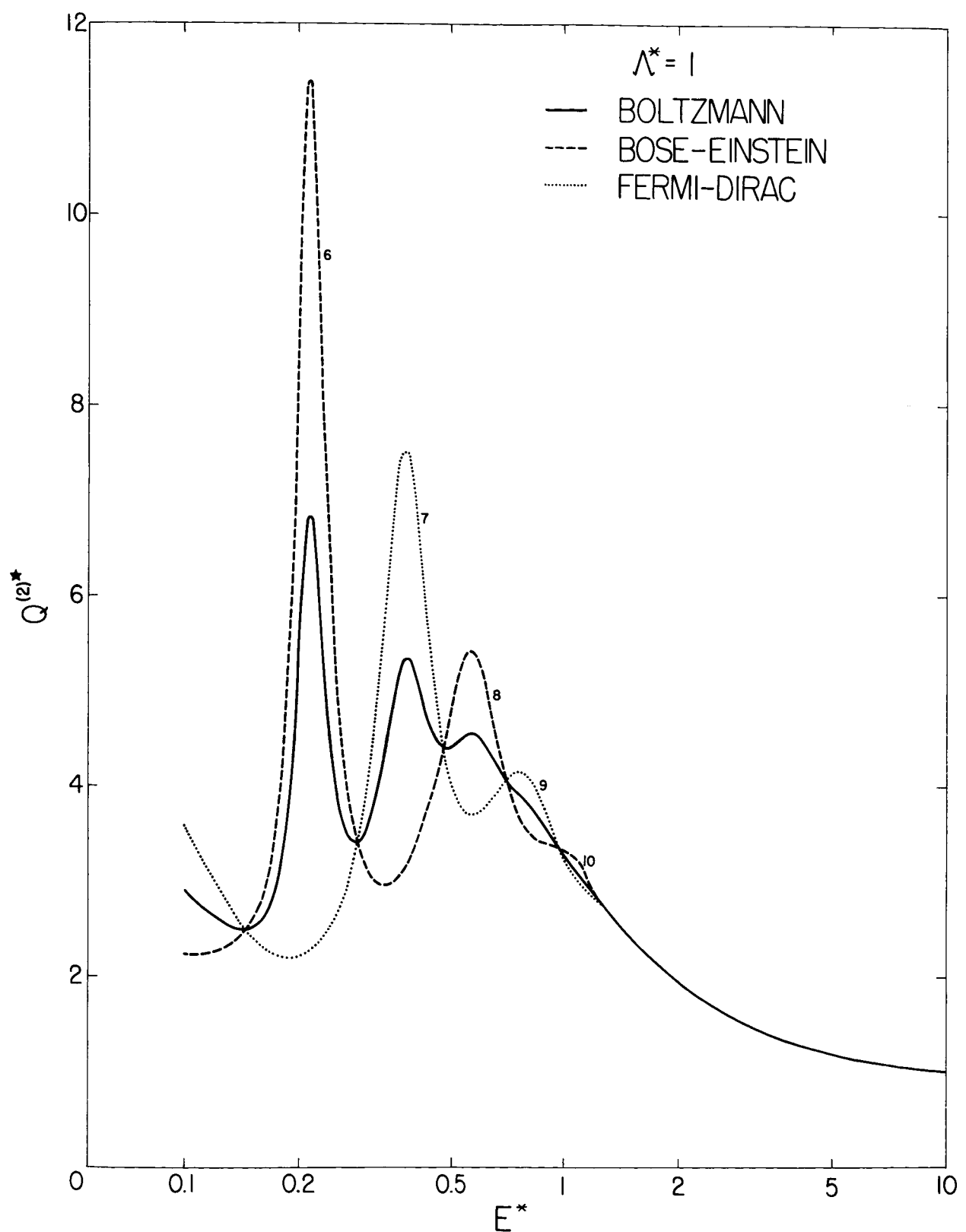
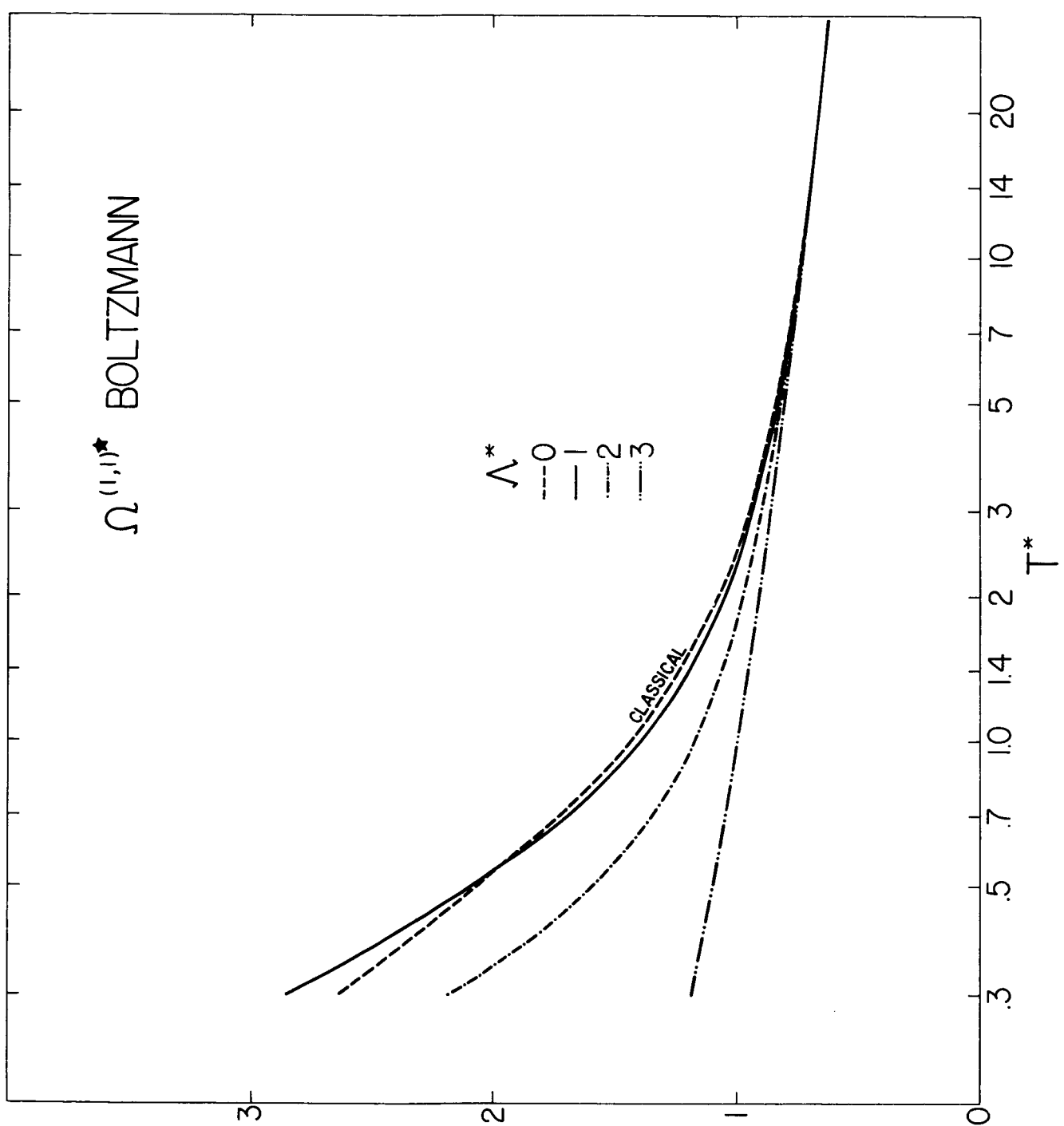


FIG. 3



$\Omega^{(1,1)}$

FIG. 4

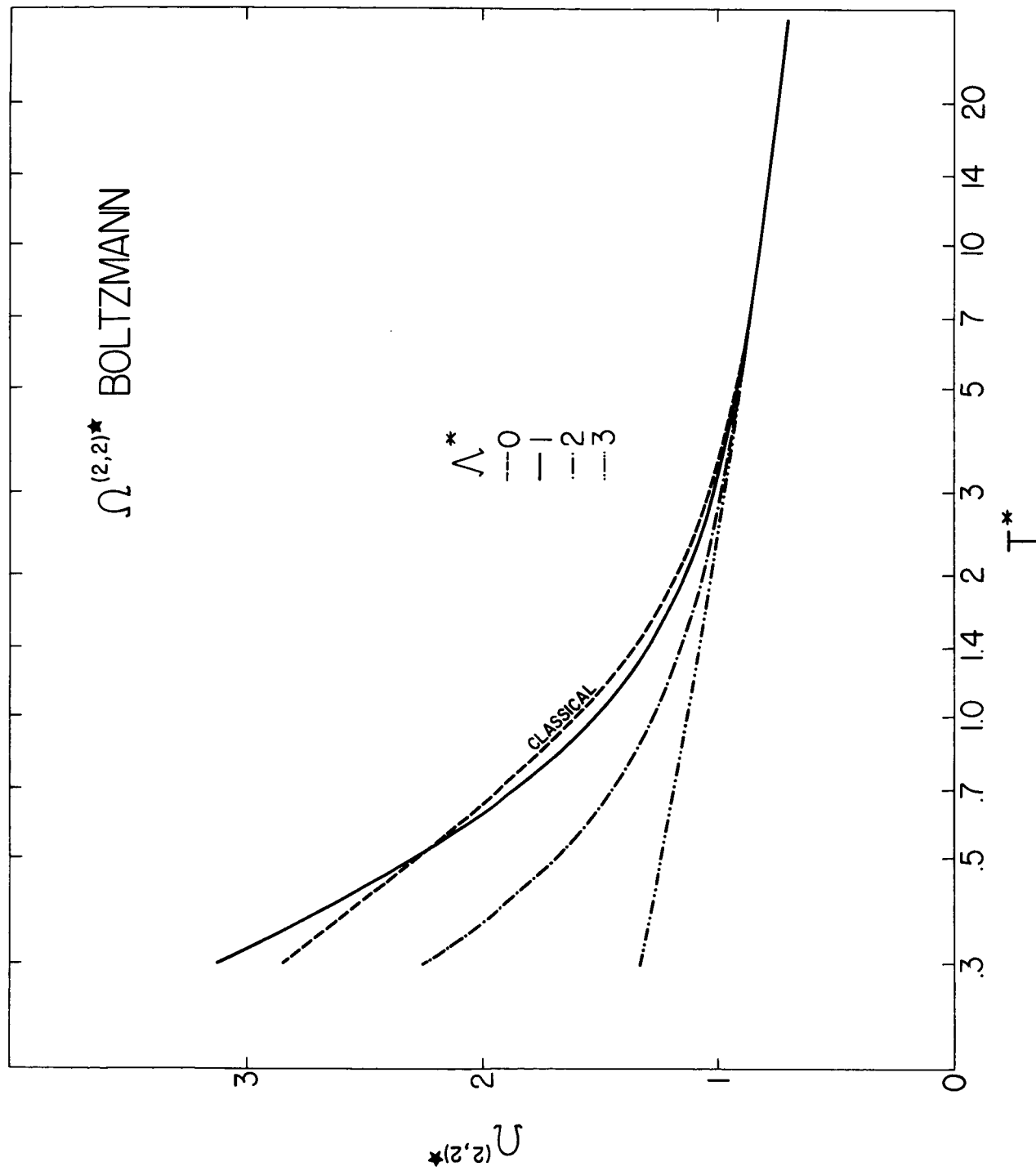


FIG. 5

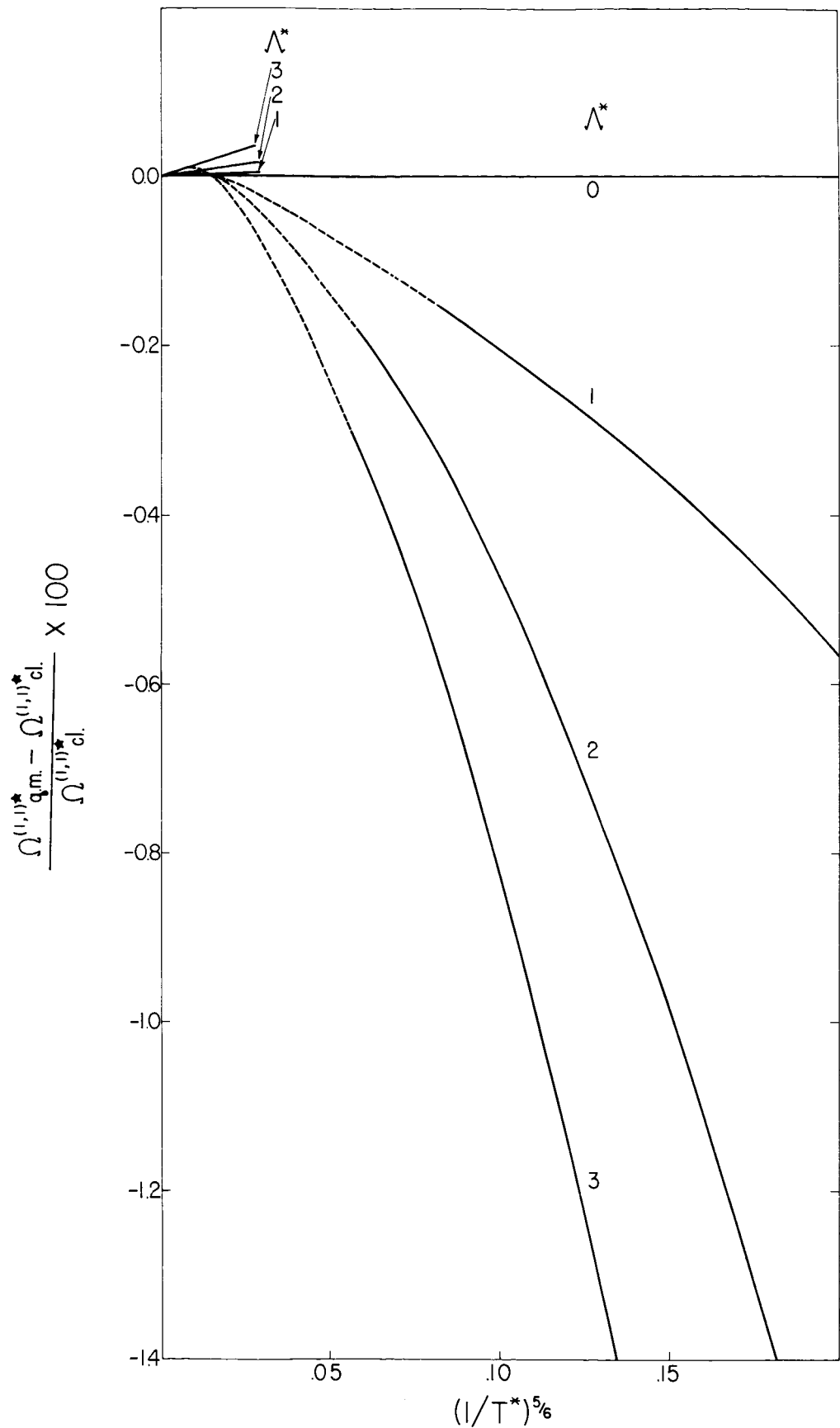


FIG. 6

FIG. 7

